

Three-Photon Excitation of *p*-Quaterphenyl with a Mode-Locked Femtosecond Ti:Sapphire Laser

Ignacy Gryczynski,¹ Henryk Malak,¹ and Joseph R. Lakowicz¹

Received November 15, 1995; accepted April 15, 1996

We observed emission from *p*-quaterphenyl (p-QT) at 360 nm when exposed to the focused light from a femtosecond (fs) Ti:sapphire laser at 850 nm. This wavelength is too long to allow two-photon excitation of p-QT. The emission intensity of p-QT was found to depend on the cube of the laser power at 850 nm, suggesting that excitation occurs due to a three-photon process. The same emission spectrum and single exponential decay times were observed for three-photon excitation at 850 nm as for two-photon excitation at 586 nm and for one-photon excitation at 283 nm. The same rotational correlation times were observed for one-, two-, and three-photon excitation, but higher time-zero anisotropies were observed for two- and three-photon excitation. The steady-state anisotropies for one-, two-, and three-photon excitation are precisely consistent with $\cos^2\theta$, $\cos^4\theta$, and $\cos^6\theta$ excitation photoselection, where θ is the angle between the electric field of the incident light and the absorption dipole. These experiments were performed with 3×10^{-5} M solutions of p-QT. Use of such low concentrations was possible because p-QT displays one of the highest apparent cross sections we have observed to date for three-photon excitation. The spatial distribution of the excited fluorescence was less for three-photon excitation than for two-photon excitation of Coumarin 102 at the same 850-nm excitation wavelength. The high cross section, photostability, and clear $\cos^6\theta$ photoselection of p-QT make it an ideal three-photon standard for spectroscopy and microscopy.

KEY WORDS: Three-photon excitation; two-photon excitation; time-resolved anisotropy; frequency domain; Ti:sapphire laser.

INTRODUCTION

Two-photon excitation of fluorescence is becoming a widely used tool in biomedical science. By two-photon excitation we mean the simultaneous absorption of two red long-wavelength photons to result after internal conversion, in excitation to the first singlet state. Two-photon excitation has been used to study the excited-state symmetry of biochemical fluorophores^(1,2) and for studies of time-resolved fluorescence.⁽³⁻⁵⁾ Other important appli-

cations of two-photon excitation are in fluorescence microscopy with localized two-photon excitation,⁽⁶⁻⁸⁾ localized release of caged compounds,⁽⁹⁾ and pattern photobleaching in fluorescence photobleaching.⁽¹⁰⁾ The fluorescence intensity from two-photon excitation is proportional to the square of the peak laser power. Consequently, the increasing availability of picosecond (ps) dye lasers and femtosecond (fs) Ti:sapphire lasers has made it possible to excite a large number of biochemical fluorophores.

In recent reports we have shown that fluorophores could be excited by three-photon excitation using the fundamental output of a fs Ti:sapphire laser. Three-photon excitation has been observed for simple fluorop-

¹ Center for Fluorescence Spectroscopy, Department of Biological Chemistry, University of Maryland School of Medicine, 108 North Greene Street, Baltimore, Maryland 21201.

Table I. Expected and Observed Anisotropies for One-, Two-, and Three-Photon Excitation

Number of photons ^a	Calculated ^b		Observed					
			5°C		20°C		-50°C	
	r_{0i}	r_{0i}/r_{01}	r_{0i}	r_{0i}/r_{01}	r_{0i}	r_{0i}/r_{01}	r_{0i}	r_{0i}/r_{01}
1	0.400	1.00	0.267	1.000	0.198	1.000	0.386	1.000
2	0.571	1.429	0.372	1.393	0.286	1.444	0.541	1.402
3	0.667	1.667	0.436	1.633	0.332	1.677	0.638	1.653

^aNumber of simultaneously absorbed photons.

^bExpected value for $\beta = 0$ in Eqs. (4)–(8).

hores,⁽¹¹⁾ the membrane probe DPH,⁽¹²⁾ for a tryptophan derivative,⁽¹³⁾ and for the calcium probe Indo-1.⁽¹⁴⁾ However, little is presently known about the spectral properties of fluorophores with three-photon excitation. In the literature there is a lack of suitable reference compounds for two- and three-photon spectroscopy and microscopy. Hence we investigated the spectral properties of *p*-quaterphenyl (p-QT) with multi-photon excitation. Depending on the wavelength, excitation of p-QT can occur via a one-, two-, or three-photon process. p-QT displays three-photon excitation above 800 nm, which is conveniently available from Ti:sapphire lasers. p-QT displays one of the largest apparent three-photon cross sections we have observed to date, making it a useful standard for three-photon excitation.

THEORY

The nature of the excitation process can be revealed by anisotropy measurements with polarized excitation. This theory has been presented elsewhere^(11,15) but is briefly reported here to allow interpretation of the anisotropy measurements.

For vertically polarized excitation the anisotropy is given by

$$r_{0i}(\theta, \beta) = \left(\frac{3}{2} \langle \cos^2 \theta \rangle_i - \frac{1}{2} \right) \left(\frac{3}{2} \cos^2 \beta - \frac{1}{2} \right) \quad (1)$$

where θ is the angle from the *z*-axis, β is the angle between the absorption and the emission transition moments, the subscript zero indicates the absence of rotational diffusion during the excited-state lifetime or the time 0 anisotropy, and *i* indicates the number of simultaneous absorbed photons. The average value of $\cos^2 \theta$ depends upon the type of photoselection. The value of

$\langle \cos^2 \theta \rangle_i$ is given by

$$\langle \cos^2 \theta \rangle_i = \frac{\int_0^{\pi/2} \cos^2 \theta f_i(\theta) d\theta}{\int_0^{\pi/2} f_i(\theta) d\theta} \quad (2)$$

where $f_i(\theta)$ is the directional distribution of the excited state.⁽¹⁵⁾ For one-photon excitation this distribution is given by

$$f_1(\theta) = \cos^2 \theta \sin \theta \quad (3)$$

For one-photon excitation Eq. (1) becomes

$$r_{01}(\beta) = \frac{2}{5} \left(\frac{3}{2} \cos^2 \beta - \frac{1}{2} \right) \quad (4)$$

where the factor of 2/5 originates with $\cos^2 \theta$ photoselection [Eq. (3)]. For collinear transitions ($\beta = 0$) the fundamental anisotropy (r_{01}) without rotational diffusion is 0.40 (Table I).

The anisotropy expected for two (r_{02})- or three (r_{03})-photon excitation can be calculated using

$$f_2(\theta) = \cos^4 \theta \sin \theta \quad (5)$$

$$f_3(\theta) = \cos^6 \theta \sin \theta \quad (6)$$

where the subscript (2 or 3) refers to two- or three-photon excitation. Substitution into Eq. (1) yields

$$r_{02}(\beta) = \frac{4}{7} \left(\frac{3}{2} \cos^2 \beta - \frac{1}{2} \right) \quad (7)$$

$$r_{03}(\beta) = \frac{2}{3} \left(\frac{3}{2} \cos^2 \beta - \frac{1}{2} \right) \quad (8)$$

For two- and three-photon excitation the maximal anisotropies for $\beta = 0$ are 0.57 (4/7) and 0.66 (2/3), respectively (Table I). Hence, for collinear transitions three-photon excitation is expected to result in a more

highly oriented excited state population. The observation of a larger anisotropy for three- versus two-photon excitation provides strong evidence for three-photon excitation. However, it is important to remember that three-photon excitation need not result in higher anisotropies, as has already been predicted⁽¹⁶⁾ and observed^(17,18) for two-photon excitation.

MATERIALS AND METHODS

p-QT was purchased from Aldrich (99.5%) and used without further purification. Coumarin 102, 99%, laser grade, was from Eastman-Kodak. For one-photon excitation of *p*-QT we used either the frequency-doubled output of a rhodamine 6G dye laser near 300 nm or the arc lamp on the steady-state fluorometer. Excitation from 570 to 600 nm was provided by the fundamental output of a rhodamine 6G dye laser, which was synchronously pumped by a mode-locked argon ion laser. The repetition rate was 3.796 MHz, with a pulse width near 6 ps, and the average power was about 100 mW. Excitation from 810 to 900 nm was provided by a fs mode-locked Ti:sapphire laser from Spectra Physics. The repetition rate of 80 MHz was held fixed by the Loc-to-Clock accessory. The repetition rate was divided by 8 by the Loc-to-Clock electronics and used as the 10 MHz reference signal for the frequency-domain (FD) instrument. The pulse width was near 80 fs and the average power was about 1 W.

The fundamental outputs of the Ti:sapphire or the dye lasers were brought directly to sample compartment and focused with a laser-quality lens (2-cm focal length). For intensity and anisotropy decay measurements the emission was isolated with a stack of two UG-11 filters which transmitted from 280 to 390 nm, combined with a short-wave pass filter. This combination of filters transmitted about 50% of the light near 350 nm (OD = 0.4). The suppression of the filter combination outside the observation region was about 10^{-8} (OD = 8). The signal of the solvent alone was less than 0.2%. The samples were stirred during the measurements, but stirring was not necessary to obtain a stable signal. Without stirring the intensity decreased about 3% during illumination. The concentration of *p*-QT in triacetin for the intensity and anisotropy decay measurements was near 3×10^{-5} M, as determined from the optical density near 1.3 at 297 nm and the extinction coefficient of 4.28×10^4 M⁻¹ cm⁻¹.⁽¹⁹⁾

FD intensity and anisotropy decays were obtained on the instrumentation described previously⁽²⁰⁾ using

magic-angle polarization conditions. FD intensity and anisotropy data were analyzed by nonlinear least squares.^(21,22) Intensity and anisotropy decays were analyzed in terms of single-exponential models,

$$I(t) = I_0 \exp(-t/\tau_i) \quad (9)$$

$$r(t) = r_{0i} \exp(-t/\phi_i) \quad (10)$$

where τ_i is the decay time, ϕ_i is the rotational correlation time, and the subscript *i* refers to the number of photons in the excitation process.

For emission spectra we used a SLM AB-2 spectrofluorometer with a 4-nm bandpass. Solutions were in equilibrium with air. The signals from the solvents alone were less than 0.1% of that observed in the absence of *p*-QT. For measurements of the dependence of the emission on laser intensity, the peak power was attenuated with neutral density filters. To avoid any effects of widening the laser pulses by the neutral density filters, a single filter of the same design and thickness, but varying optical density, was used for the intensity measurements at various peak powers. All measurements were performed in triacetin at room temperature, near 20°C, except for the frozen solution anisotropies, which were measured at -50°C. The steady-state anisotropies, were also measured at 5°C for different modes of excitation.

In the presence of rotational diffusion the steady-state anisotropy (r_i) is lower than the time 0 anisotropy. The steady-state anisotropy is related to the value of r_{0i} and to the rotational correlation time (ϕ_i) by

$$\frac{r_{0i}}{r_i} = 1 + \frac{\tau}{\phi_i} \quad (11)$$

where τ is the decay time.

RESULTS

Emission spectra are shown in Fig. 1 for *p*-QT excited at 850 nm (dashed line). We were surprised by emission at this long excitation wavelength. Two-photon excitation of *p*-QT is not expected because its one-photon absorption is near zero above 350 nm,⁽¹⁹⁾ so that two-photon excitation is not expected above 700 nm. The emission spectrum observed with 850-nm excitation is essentially identical to that found with one-photon excitation at 283 nm (Fig. 1, solid line). To determine the nature of excitation at 850 nm the intensity of the laser beam was attenuated two-fold. This attenuation resulted in an eight-fold decrease in emission intensity, which implies a three-photon process. At 850 nm the emission

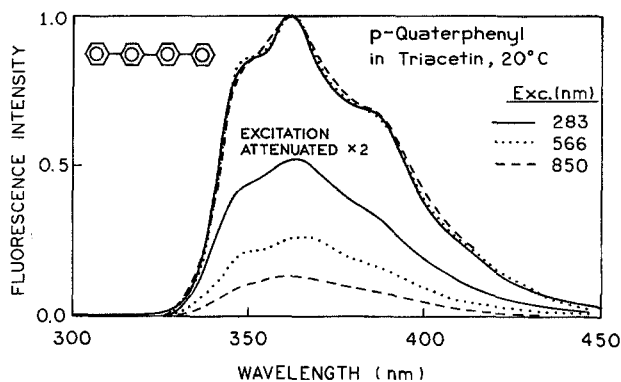


Fig. 1. Emission spectra of *p*-quaterphenyl for excitation at 283 nm (—), 566 nm (.....), and 850 nm (---). Also shown are the emission spectra recorded with a twofold attenuation of the incident light.

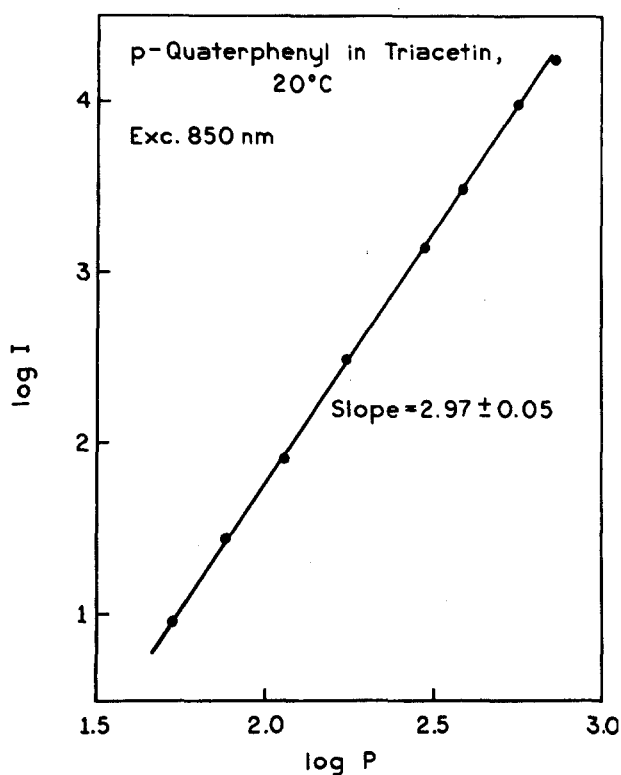


Fig. 2. Dependence of the emission intensity of *p*-quaterphenyl in triacetin on the incident power at 850 nm from the Ti:sapphire laser. The laser power (P) is in milliwatts.

intensity of *p*-QT was found to depend almost precisely on the cube of the laser power (Fig. 2). At the shorter wavelength of 566 nm a twofold attenuation of the incident light results in a fourfold decrease in *p*-QT intensity (Fig. 1, dotted line), indicating two-photon excitation at this wavelength.

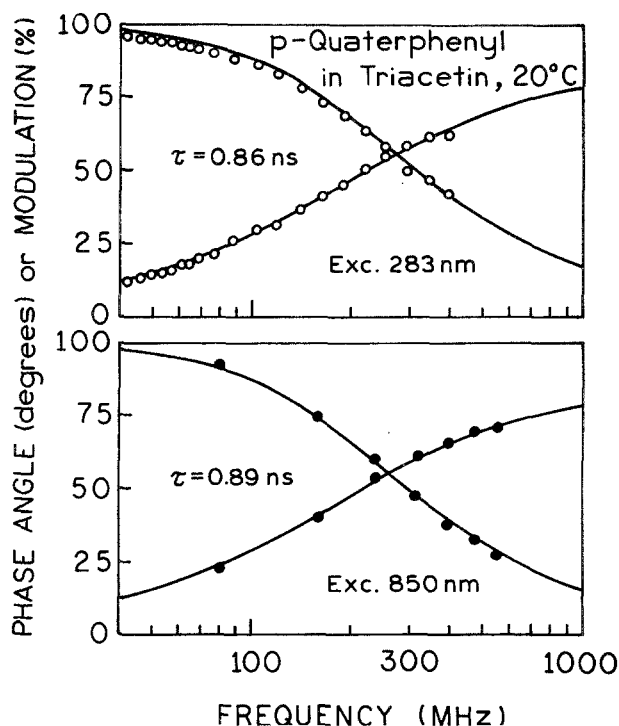


Fig. 3. Frequency-domain intensity decay of *p*-quaterphenyl in triacetin, 20°C, for excitation at 283 nm (top) and 850 nm (bottom).

Table II. Intensity and Anisotropy Decays of *p*-Quaterphenyl in Triacetin at 20°C

Excitation (nm)	τ (ns)	r^a	r_0^b	ϕ (ns) ^b	r_0^c
283	0.86	0.198	0.371	0.93	0.386
566	0.85	0.286	0.540	0.96	0.541
850	0.87	0.332	0.639	0.97	0.638

^aSteady-state anisotropy.

^bRecovered from the frequency-domain anisotropy decay.

^cMeasured in triacetin at -50°C.

To characterize further the emission of *p*-QT with long-wavelength excitation, we examined the intensity decays using the FD method. Precisely the same decay time for *p*-QT was observed for excitation at 283 and 850 nm in triacetin (Fig. 3) and for two-photon excitation at 566 nm (Table II). The similarity of the intensity decay suggests that the sample is not being significantly perturbed by the intense illumination at 850 nm (Table II).

FD anisotropy decay data for *p*-QT in triacetin are shown in Fig. 4. The similar shape of the differential phase data suggest similar correlation times for one- and three-photon excitation at 283 and 850 nm, respectively.

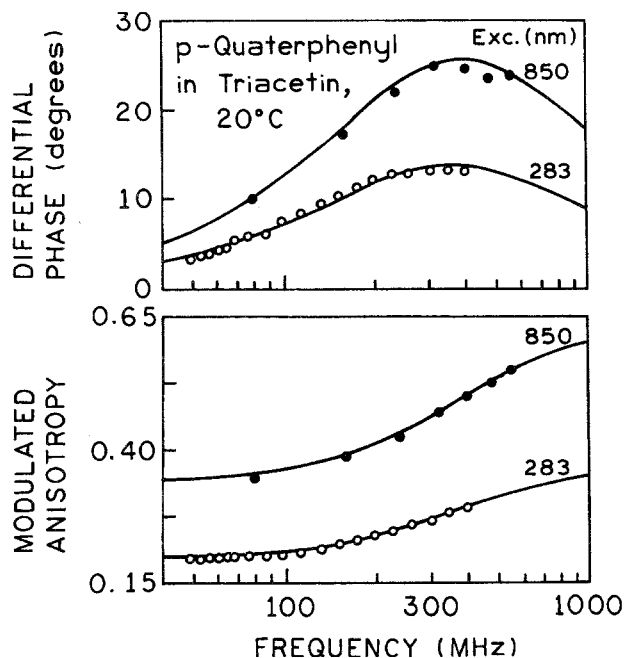


Fig. 4. Frequency-domain anisotropy decays of *p*-quaterphenyl in triacetin, 20°C, for excitation at 283 nm (●) and 850 nm (○).

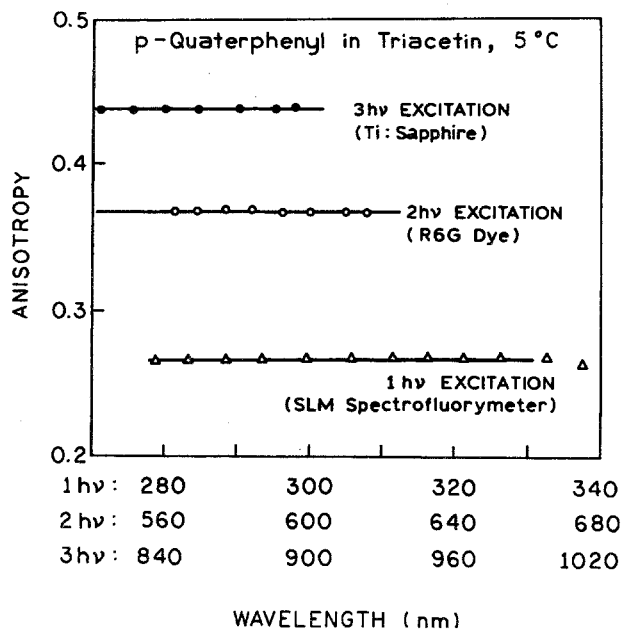


Fig. 5. Excitation-dependent steady state anisotropies for one (Δ)-, two (○)-, and three (●)-photon excitation of *p*-quaterphenyl at 5°C.

The larger values of the differential phase angles and modulated anisotropies suggest higher time 0 anisotropies for three-photon excitation. The data were used to calculate the rotational correlation time (ϕ_i) and time 0

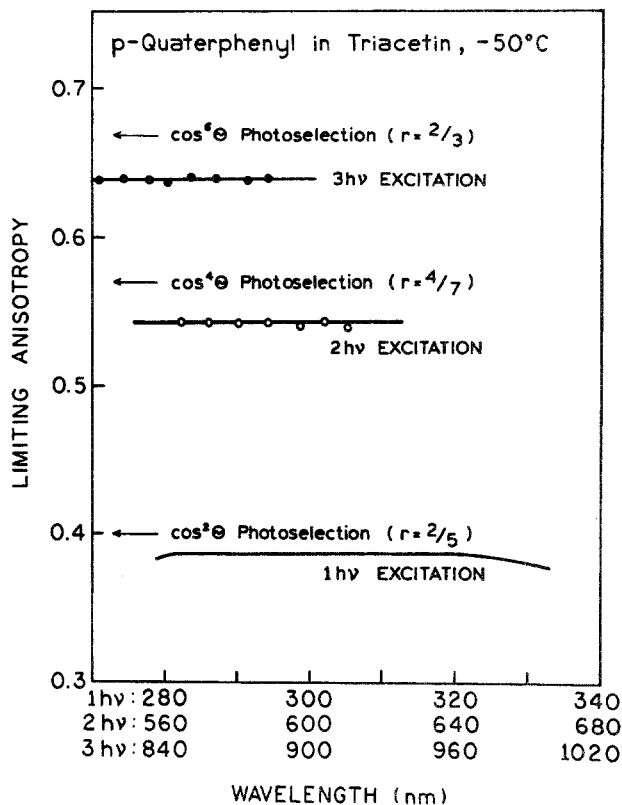


Fig. 6. Fundamental anisotropies of *p*-quaterphenyl (triacetin, -50°C) for one (—), two (○)-, and three (●)-photon excitation of *p*-quaterphenyl.

anisotropy (r_{01} and r_{03}) for one-, two-, and three-photon excitation, respectively (Table II). The correlation times were identical, again indicating the absence of significant heating or sample perturbation. However, the time 0 anisotropy is $r_{01} = 0.371$ for one-photon excitation, $r_{02} = 0.540$ for two-photon excitations and $r_{03} = 0.639$ for three-photon excitation, which indicates a more highly oriented excited-state population with two- and three-photon excitation.

To characterize further *p*-QT as a standard for multiphoton excitation, we examined its steady-state anisotropies for a range of excitation wavelengths, from 280 to 900 nm. Steady-state anisotropy measurements were performed in triacetin at 5°C (Fig. 5) and at -50°C, where rotational diffusion does not occur during the excited-state lifetime (Fig. 6). We observed nearly constant anisotropies in each wavelength region for one (280- to 340-nm)-, two (560- to 620-nm)-, and three- to (810 to 870-nm)-photon excitation. The anisotropy values scale precisely according to $\cos^2\theta$, $\cos^4\theta$, and $\cos^6\theta$ photoselection (Table II). This result indicates that the transition tensor for *p*-QT is dominated by a single element for all modes of excitation.

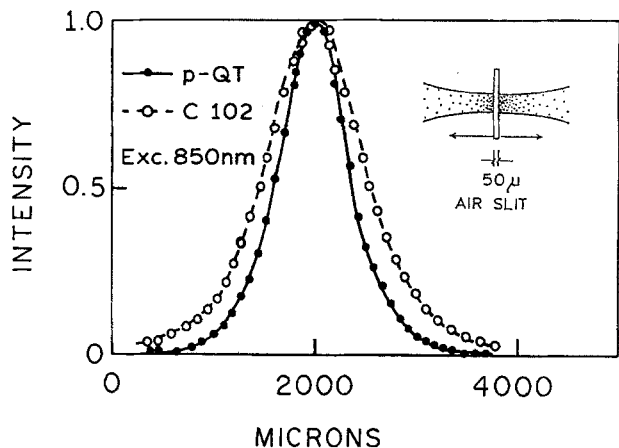


Fig. 7. Spatial distribution of the emission of *p*-querphenyl with three-photon excitation (●) and coumarin (C) 102 with two-photon excitation (○), both with 850-nm excitation.

An important characteristic of two-photon excitation for fluorescence microscopy is localization of the excited fluorophores at the focal point, with minimal excitation above and below the focal plane.⁽⁶⁻⁸⁾ Hence we decided to determine if three-photon excitation provided still more strongly localized excitation. We examined the spatial distribution of the excited fluorophores by observation with an optical fiber positioned on a 50- μm vertical slit, 3 mm high (Fig. 7). We compared the spatial distribution of the emission of *p*-QT with three-photon excitation with that shown for coumarin 102, which displayed two-photon excitation at the same 850-nm excitation wavelength.

The excited region of the sample is localized with two-photon excitation at 850 nm (Fig. 7). Three-photon excitation at 850 nm results in still more strongly localized excitation, with almost no emission 500 μm from the focal region. These data seem to exclude harmonic generation in the sample, followed by absorption of the harmonic by *p*-QT. In this case the spatial profile would be less symmetrical because the harmonic would excite *p*-QT deeper in the sample. While the precise spatial distribution of the fluorescence depends on the particular optics used for focusing and excitation, it seems clear that strongly localized fluorescence can be obtained with three-photon excitation (Fig. 7).

It is important to note that these experiments were performed using $3 \times 10^{-5} M$ *p*-QT. The use of such a dilute solution was possible because of the high apparent cross section displayed by *p*-QT for three-photon excitation. While we are not able to quantify the numerical value of the three-photon cross section, the signal from *p*-QT is about 100-fold larger than that observed for

DPH in the same solvent under comparable conditions.⁽¹²⁾ For this reason we feel that *p*-QT can be useful as a test substance whenever one is starting an experiment in three-photon spectroscopy or microscopy.

DISCUSSION

The results presented above indicate that *p*-QT is a rather ideal standard for multiphoton excitation. By selection of the wavelength it can be excited by either two or three photons. This multiphoton excitation can be accomplished in dilute solution, near $10^{-5} M$, where inner filter effects are not significant. The intensity and anisotropy decays are single exponentials independent of the mode of excitation. The steady-state and time 0 anisotropies scale precisely according to $\cos^2\theta$, $\cos^4\theta$, and $\cos^6\theta$ photoselection. This means that one can use the one-photon anisotropy observed in a cuvette to predict the expected value for two- or three-photon excitation in a microscope. According to our best knowledge, the three-photon anisotropy value of 0.638 (Table II) is the highest measured fluorescence anisotropy reported for isotropic solution.

An additional advantage of three-photon excitation is the smaller excited volume. By comparison of the emission from cuvettes containing fluorophores which display two- or three-photon excitation, we showed that the emission is seen from a smaller area for three-photon excitation. These spatial profiles suggest that higher spatial resolution can be obtained by three-photon excitation in fluorescence microscopy. Three-photon excitation of 2,5-bis(4-biphenyl)oxazole (BBO) has already been observed in a microscope.⁽²³⁾

ACKNOWLEDGMENTS

This work was supported by NIH National Center for Research Resources Grants RR-08119 and RR-10416. The authors thank Spectra Physics and, especially, Mr. Alan Del Gaudio, Mr. Gary Eisenman, and Mr. Bob Letique for the loan of the Ti: sapphire laser used for these experiments.

REFERENCES

1. R. R. Birge (1986) *Acc. Chem. Res.* **19**, 138-146.
2. B. Hudson and B. Kohler (1974) *Annu. Rev. Phys. Chem.* **25**, 437-460.
3. J. R. Lakowicz, I. Gryczynski, J. Kuéba, and E. Danielsen (1992) *J. Fluoresc.* **2**, 247-258.

4. J. R. Lakowicz and I. Gryczynski (1992) *J. Fluoresc.* **2**, 117–122.
5. J. R. Lakowicz and I. Gryczynski (1993) *Biophys. Chem.* **45**, 1–6.
6. W. Denk, J. H. Strickler, and W. W. Webb (1990) *Science* **248**, 73–76.
7. S. W. Hell, S. Lindek, and E. H. K. Stelzër (1994) *J. Modern Optics* **41**(4), 675–681.
8. W. Denk (1994) *Proc. Natl. Acad. Sci. USA* **91**, 6629–6633.
9. W. Denk, K. R. Delaney, A. Gelperin, D. Kleinfeld, B. W. Strowbridge, D. W. Tank, and R. Yuste (1994) *J. Neurosci. Meth.* **54**, 151–152.
10. Z. Huang and N. L. Thompson (1993) *Biophys. Chem.* **47**, 241–249.
11. I. Gryczynski, H. Malak, and J. R. Lakowicz (1995) *Chem. Phys. Lett.* **245**, 30–35.
12. I. Gryczynski, H. Malak, J. D. Dattelbaum, and J. R. Lakowicz (1996), *J. Fluorescence*, in press.
13. I. Gryczynski, H. Malak, and J. R. Lakowicz (1996) *Biospectroscopy* **2**, 9–15.
14. I. Gryczynski, H. Szmajnski, and J. R. Lakowicz (1995) *Photochem. Photobiol.* **62**, 804–808.
15. J. R. Lakowicz, I. Gryczynski, Z. Gryczynski, E. Danielsen, and M. J. Wirth (1992) *J. Phys. Chem.* **98**, 3000–3006.
16. P. R. Callis (1993) *J. Chem. Phys.* **99**(1), 27–37.
17. J. R. Lakowicz, I. Gryczynski, E. Danielsen, and J. K. Frisoli (1992) *Chem. Phys. Lett.* **194**, 282–287.
18. J. R. Lakowicz, B. Kierdaszuk, P. Callis, H. Malak, and I. Gryczynski (1996) *Biophys. Chem.* (in press).
19. I. B. Berlman (Ed.) (1971) *Handbook of Fluorescence Spectra of Aromatic Molecules*, Academic Press, New York.
20. G. Laczko, J. R. Lakowicz, I. Gryczynski, Z. Gryczynski, and H. Malak (1990) *Rev. Sci. Instrum.* **61**, 2331–2337.
21. E. Gratton, J. R. Lakowicz, B. Maliwal, H. Cherek, G. Laczko, and M. Limkeman (1984) *Biophys. J.* **46**, 479–486.
22. J. R. Lakowicz, H. Cherek, J. Kuśba, I. Gryczynski, and M. L. Johnson (1993) *J. Fluoresc.* **3**, 103–116.
23. S. Hell, M. Schrader, K. Bahlmann, F. Meinecke, J. R. Lakowicz, and I. Gryczynski (1995) *J. Microsc.* **180**(2), RP1–RP2.